SHORT THESIS FOR THE DEGREE OF DOCTOR OF PHILOSOPHY (PHD)

Agonist binding directs dynamic competition among nuclear receptors for heterodimerization with their common partner, retinoid X receptor

By: Lina Fadel, Pharm D, MS

Supervisor: György Vámosi, PhD

University of Debrecen

Doctoral school of Molecular Medicine

Debrecen, 2022

Agonist binging directs dynamic competition among nuclear receptors for heterodimerization with their common partner, retinoid X receptor

By **Dr. Lina Fadel, Pharm D**
Supervisor: **Dr. György Vámosi, PhD**

Doctoral School of Molecular Medicine, University of Debrecen

Head of the Defense Committee:	Prof. László Csernoch, PhD, DSc
Reviewers:	Dr. Szilvia Benkő, PhD
	Dr. Tibor Pankotai, PhD
Members of the Defense Committee:	Dr. Lajos Széles, PhD
	Dr. Tamás Hegedűs, PhD

The PhD defense takes place online via Zoom at 10 AM, 24th March 2022.

To participate at the defense, please request the Zoom link from biophys@med.unideb.hu before 4PM CET on 23/3/2022.

1. INTRODUCTION

Nuclear receptors (NR) are a superfamily of structurally related proteins and serve as the largest group of transcription factors in eukaryotes. They exert their transcriptional activity as a response to binding to their ligands; hence they are classified as ligand dependent transcription factors.

This family of receptors comprises 49 NRs in humans, and they sense a wide variety of ligands e.g., steroids, hormones, vitamins, metabolites, xenobiotics, and many new ones are continuously being recognized.

Through binding to their ligands, NRs control a vast variety of biological process like development, cell differentiation, metabolism and cell death. Consequently, dysfunctions in these pathways may end up with critical pathological issues ranging from simple metabolic diseases to cancers. Governing important signaling pathways spotlighted nuclear receptors as important druggable targets and a plethora of studies have been focusing on this field.

Nuclear receptors share a common structure composed of several functional domains: a ligand-independent N-terminal transcription activation function domain (AF-1), a DNA-binding domain (DBD), a flexible hinge region and a ligand-binding domain (LBD) also functioning as a ligand-dependent transcription activation function domain (AF-2) at the C terminus. The main function of the DBD is to bind to a specific DNA sequence called a hormone response element (HRE).

Among NRs, retinoid x receptor (RXR) serves as an obligatory heterodimerization partner for at least 20 other NRs like the peroxisome proliferator-activated receptor gamma, PPARγ, the retinoid acid receptor alpha, RARα, and vitamin D receptor, VDR.

RXR-NRs heterodimers recognize HRE-s composed of two AGGTCA half-sites arranged as direct repeats (DRs) and separated by a spacer of zero to eight base pairs termed DR0 to DR8.

Moreover, the DBD also contributes to receptor heterodimerization, and it harbors between its two zinc finger motifs a nuclear localization signal termed NLS1 mediating the nuclear localization of the receptors. The LBD accommodates the core of NR actions since it contains the ligand-binding pocket and regions that mediate dimer formation, coregulator binding and ligand-dependent transactivation.

The mechanism of activation called molecular switch is also a common characteristic of these receptors. In the absence of the cognate ligand, the heterodimeric complex of RXR and its partner

binds to DNA in its “apo” form and recruits corepressors leading to a transcriptionally repressed state. The liganded receptors change their conformation to their “holo” form, which reduces their affinity for corepressors and leads to coactivator binding and transcription initiation. This similarity in structure, mechanism of activation and sharing of coregulators suggest a potential crosstalk between the members of this NR family and a competition for the common binding partners, i.e., for RXR, coactivator or DNA binding sites.

Numerous fluorescence microscopy studies have analyzed the molecular mechanism of NR activation by observing protein-protein and protein-DNA interactions and dynamics. Homodimerization of RXR-LBD is enhanced upon 9-cis-retinoic acid treatment as demonstrated by fluorescence fluctuation analysis. Previously we have shown by fluorescence correlation spectroscopy that specific agonists increase chromatin binding of RARα and RXRα in a coactivator dependent manner. We have shown by light sheet microscopy-based Förster resonance energy transfer and fluorescence cross-correlation measurements (SPIM-FRET-FCCS) that dimerization of RARα and RXRα and chromatin binding of the dimer are enhanced upon agonist treatment.

Typically, multiple heterodimeric partners of RXR are present in certain cell types. In cells where there is a limiting or sequestered pool of RXR combined with the expression of several RXR heterodimerization partners, the mechanism by which RXR partner selection is mediated remains unclear. We hypothesized that there is a competition between RXR partners for binding to RXR and that binding of a specific agonist increases the affinity of a given receptor to RXR and favors their heterodimerization. RXRα and three NR partners were included in this study: PPARγ, VDR and RARα.

The present work was undertaken to better understand RXRα partitioning between its different heterodimeric partners in the absence and presence of their cognate agonists. This may have pharmacological implications by improving the current usage of the present drugs in triggering specific signaling pathways and may explain how targeting one NR pathway can interfere with a seemingly distinct NR pathway.

2. OBJECTIVE

In cells where there is a limiting or sequestered pool of RXR combined with the expression of several RXR heterodimerization partners (NRs), the mechanism of RXR partner selection remains unclear. Previous data suggested that specific agonist treatment could enhance heterodimerization and chromatin binding of RXR and RAR. We aimed to answer the following questions:

I. **Is there competition between RXR partners for binding to RXR?**
II. **Does binding of a specific agonist increase the affinity of a given receptor to RXR and favor their heterodimerization?**
III. **What is the effect of specific agonist treatment on the direct DNA binding of NRs?**

To study these questions, we developed a nuclear translocation assay for monitoring the heterodimerization of RXR and its NR partners specifically; PPARγ, VDR and RARα, and competition was detected at different treatment conditions: in the absence of external ligand, upon treatment with a single specific agonist (of one partner) and upon cotreatment with specific agonists of the two competing partners.

Chromatin immunoprecipitation sequencing was applied to unravel the changes in the genomic binding sites of VDR upon specific agonist treatment.

Better understanding of RXRα partitioning between its different heterodimeric partners may help to improve the therapeutic application and reduce the side effects of drugs triggering different specific signaling pathways and explain how targeting an NR pathway can interfere indirectly with a seemingly distinct NR pathway.

Intercalators like doxorubicin influence the superhelicity and dynamics of chromatin, which may affect the binding of nuclear proteins to their specific response elements. Previous studies have suggested that treatment with specific RAR agonists like ATRA could reduce the cardiotoxicity of Doxorubicin and increase its efficacy. Thus, we set out to investigate:

IV. **How does doxorubicin affect the DNA binding of RARα?**

To this end, we monitored mobility changes of RARα upon treatment with different doses of doxorubicin, in the absence or presence of specific RARα agonist. Changes in DNA-binding of NRs may interfere with their transcriptional activities and could account in part for the side effects caused by doxorubicin.

3. Materials and Methods

3.1. Plasmid construction

EGFP-NRs (PPARγ, RARα, and VDR) were cloned using their human cDNA, splice variant (isoform) 1 as templates and pCMV-EGFP-C3 as a vector. mCherry-NRs were generated from EGFP tagged receptors by replacing EGFP with mCherry. Candidate NLS-s in the DBDs of the involved NRs have been mutated using site-directed mutagenesis via the overlap extension PCR method. BFP-RXRα/*nlsm* was generated from EGFP-RXRα/*nlsm* by replacing EGFP-C3 with tag-BFP-C3 using NheI and BglII restriction enzymes. Zinc finger mutant RXR, RXR/*znm*, was prepared by mutating all the 8 cysteines within the two zinc finger motifs of the DBD to alanines.

Control plasmids: EGFP-mCherry (GC^+), EGFP-BFP (GB) fusion protein are complemented with a 6 amino acids linker sequence after the sequence of EGFP. EGFP-P30-mCherry (GC^-) and TagBFP-P30-EGFP (B-P30-G) construct, the linker is 17 amino acids then a proline spacer (30 repeats, mixed from the 4 proline codons).

3.2. Generation of BFP-RXRα stable cell line

The adherent version of human embryonic kidney (HEK293) cell line stably expressing BFP-RXRα, $HEK293^{B\text{-}RXR\alpha}$, was prepared using viral transduction.

3.3. Cell culture and transient transfection

Both HEK293 and $HEK293^{B\text{-}RXR\alpha}$ were maintained in Dulbecco's Modified Eagle's Medium (DMEM), supplemented with phenol red, 10% fetal bovine serum (FBS), 1× Glutamax, 50 mg/l Gentamycin. For microscopy experiments, HEK293 or $HEK293^{B\text{-}RXR\alpha}$ cells were sub-cultured in 8-well chambered coverslips and maintained in phenol-red-free DMEM and supplemented with 10% charcoal-stripped FBS. 24 h after seeding, cells were transiently transfected with 75-80 ng of either one RXR partner (NR1) or with two competing partners (NR1+ NR2) using FuGENE® HD transfection reagent.

3.4. Ligand treatment

Ligands were applied 30-60 min before imaging at 37°C, 5% CO_2; rosiglitazone, a PPAR agonist (RSG, 1 μM); AM580, an RAR agonist (100 nM); calcitriol, a VDR agonist (100 nM); LG268, an RXR agonist (100 nM); and GW9662, a PPARγ specific antagonist (1 μM).

3.5. Microscopy

Confocal images were recorded by a Zeiss LSM 880 confocal microscope using a 40× NA 1.2 water immersion objective. The following lasers and emission filters were used: for TagBFP (Ex: 405 nm, Em: 429-481 nm), for EGFP (Ex: 488 nm, Em: 499-562 nm), and for mCherry (Ex: 543 nm, Em: 561-735 nm). An incubator built around the microscope maintained the temperature at 37°C during the measurements.

3.6. Analysis of microscopy data

The average intensity per pixel was measured in two separately, manually selected regions of interest, one contouring the entire cytoplasm and another contouring the entire nucleus, excluding the nucleoli. The values were corrected for background by subtracting the mean intensity calculated for non-transfected wt HEK293 cells. The intensities were determined using the open-source FIJI distribution of ImageJ (version 2.0.0-rc-69/1.52i). Data were presented as a ratio of nuclear-to-cytoplasmic fluorescence intensities (NCR). Analysis of variance was used to compare the differences between the groups. Prism 8.4.0 was used for statistical analysis and graphs.

3.7. Single Plane Illumination Microscopy (SPIM)

A simultaneous mapping of molecular proximity and co-mobility of RXR homodimers were assessed by measuring Förster resonance energy transfer, FRET, and Fluorescence (Cross-Correlation Spectroscopy, F(C)CS, between RXR-LBDs using a SPIM microscope and Hela cells transiently cotransfected with G-RXR-LBD and C-RXR-LBD. The calculated parameters are the FRET efficiency (E) and the relative cross-correlation function amplitude (*rCCF*), respectively.

Fluorescence was collected by a 60× NA 1 water immersion objective. Images were spectrally split to two color channels (500-550 nm, >593 nm) to detect EGFP and mCherry emission by an Andor iXon X3 860 EMCCD camera at a frame time of 530 µs, and an EM gain of 300 for F(C)CS. A 51 µm × 8 µm (128 × 20 pixel) rectangular region was imaged. In SPIM, a ~1.3 µm thin slice within the detection focal plane is illuminated by overlapping 488 and 561nm light sheets. For FCCS two different data acquisition schemes were used: first, continuous (and simultaneous) excitation by both lasers, and secondly, alternating laser excitation (ALEX) by the two lasers.

3.8. Chromatin immunoprecipitation (ChIP)

The human monocytic cell line THP-1 was maintained in RPMI medium supplemented with 10% FBS 1× GlutaMAX, 50 mg/liter gentamycin. 60 min prior to ChIP assay, THP-1 cells were maintained in phenol red-free RPMI supplemented with 10% charcoal-stripped FBS and treated with either vehicle, 1:1 DMSO–ethanol, or calcitriol (100 nM). A mouse monoclonal anti-VDR antibody was applied.

TruSeq ChIP library systems (Illumina) were used for library preparation according to the manufacturer's instructions.

Raw ChIP-seq reads were aligned to the hg19 reference genome, and BAM files were generated with SAMtools (v1.7). Peaks were predicted with the findPeaks program of the HOMER toolkit. Peaks were divided into three groups based on the presence or absence of the VDRE or NR half-site. *De novo* motif enrichment analyses were carried out with HOMER's *findMotifsGenome* and were performed on the central 200-bp regions of the peaks.

ChIP-seq data are available under accession numbers PRJNA632899 and GSE150652.

3.9. Fluorescence recovery after photobleaching, FRAP

FRAP was used to detect the effect of Doxorubicin (Dox) on the mobility of RAR. 2 hours at 37 ºC before imaging Dox was applied either alone (at 0, 1.125, 4.5, or 18 µM) or in combination with 0.1 µM AM580. Experiments were carried out in Hela cells stably expressing EGFP-RAR.

FRAP measurements were performed on a Zeiss LSM 880 confocal microscope using a 40× NA 1.2 water immersion objective. The 488 nm laser line was used to excite EGFP with and emission was detected through a 493 to 529 nm band pass filter. For quantitative analysis, a 256×256-pixel area was selected and scanned with an open pinhole (5.56 Airy units) and 10× zoom (pixel size: 0.08 µm), with a pixel dwell time of 1.33 µs. A 405-nm laser was used to bleach the EGFP molecules at a selected stripe-shaped region of interest (FRAP ROI) having an area of 140 × 10 pixels, a laser power of 20 µW at the objective, and a pixel dwell time of 8.24 µs.

Before bleaching, 10 images were collected followed by one bleach period at the FRAP ROI, and then collecting 189 post-bleach images for a total time of 42 seconds.

Images were analyzed using the ZEN software, intensities were normalized with the FRAPCalc-EMBL module, and the graphs were fitted using GraphPad Prism 8.

4. Results

4.1. Competition between RXR partners and the impact of specific agonist treatment.

We hypothesized that competition for heterodimerization with RXR is dictated, by the availability of the partner-specific agonist. To examine this hypothesis, we developed a robust system relying on a nuclear-translocation assay applied in a three-color imaging model system by detecting changes in heterodimerization between RXRα and one of its partners (NR1), in the presence of another competing partner (NR2). To this end, NR1 was present in a form showing homogeneous distribution when expressed alone and translocating into the nucleus when interacting with RXRα, and it was tagged with a green fluorescent protein; EGFP (G-). NR2 was used in its wt form and tagged with a red fluorescent protein; mCherry (C-).

First, we needed to minimize the impact of endogenously expressed NRs on the observed results. According to RNA-seq data, we chose wt HEK-293 cells and generated a stable cell line overexpressing BFP-RXRα, HEKB$^{B\text{-}RXR\alpha}$.

We transfected both wt HEK293 and HEK293$^{B\text{-}RXR\alpha}$ cell lines with G-NRs. G-PPARγ and G-RARα were localized mainly in the nucleus even in the absence of exogenously added RXRα or agonist. To impede the nuclear transport of these NRs in the absence of RXRα, we induced a mutation in the nuclear localization signal localized in their DBD between the two zinc finger motifs, NLS1. This mutation is denoted as /*nlsm*.

Then, we observed the subcellular distribution of these NLS mutant receptors (G-PPARγ/*nlsm*, G-RARα/*nlsm*) in wt HEK293 cells and studied the effect of specific agonist treatment (RSG and AM580, respectively) on their localization. The nuclear-to-cytoplasmic ratio (NCR) for G-PPARγ/*nlsm* and G-RARα/*nlsm* were ~1 irrespective of ligand treatment.

Next, we transfected the NLS mutant receptors into HEK293$^{B\text{-}RXR\alpha}$ cells to see the effect of dimerization with RXRα on their localization. We detected a 6-fold enrichment in the nucleus for G-PPARγ/*nlsm* and 5-fold for G-RARα/*nlsm*. Specific agonist treatment caused a further increase in the nuclear accumulation of these receptors.

Contrary to both G-PPARγ and G-RARα, G-VDR was distributed in wt HEK293 cell with an NCR of ~2. Treatment with a specific agonist, calcitriol, or co-expression of RXRα (using HEK293$^{B\text{-}RXR\alpha}$ cells) enhanced the translocation of G-VDR to the nucleus, resulting in an NCR value of ~3. Expressing G-VDR in HEK293$^{B\text{-}RXR\alpha}$ combined with calcitriol treatment led to an

even higher NCR value of ~6. Because wt VDR showed an increased localization in the nucleus in the presence of RXRα, it could be used in its wt form to detect heterodimerization with RXRα.

Competition between PPARγ and RARα for binding to RXRα was assessed by detecting the distribution changes of G-PPARγ/*nlsm* (NR1) in HEK293$^{B\text{-}RXR\alpha}$ in the presence of C-RARα (NR2) and cognate agonists. The nuclear accumulation of G-PPARγ/*nlsm* in HEK293$^{B\text{-}RXR\alpha}$ was dramatically reduced when cells were additionally co-transfected with C-RARα; G-PPARγ/*nlsm* became homogeneously distributed with an NCR value of around 1, similar to the case when G-PPARγ/*nlsm* was expressed alone in wt HEK293. Treatment with RSG caused a 4-fold nuclear enrichment of G-PPARγ/*nlsm*, whereas AM580 or LG268 (RXR agonist) treatment kept G-PPARγ/*nlsm* homogeneously distributed.

We co-treated these triply transfected cells with RSG, the agonist of the weak partner, at its saturating dose (1μM) and titrated AM580, the ligand of the dominant partner, from 0 to saturation, 100 nM. RSG dependent nuclear enrichment of G-PPARγ/*nlsm* in HEK293$^{B\text{-}RXR\alpha}$ cotransfected with C-RARα was abolished gradually with increasing doses of AM580.

The challenge was to prove that the dominance of RARα over PPARγ in competing for RXRα was not due to expressing mutant PPARγ and intact RARα; therefore, a complementary experiment was also carried out. Here, G-RARα/*nlsm* served as NR1 the changes in its nuclear localization were detected in HEK293$^{B\text{-}RXR\alpha}$ in the presence of C-PPARγ as an NR2. The results were consistent with our previous observation; in the absence of an agonist, RARα has a higher binding affinity to RXRα than PPARγ while treatment with specific PPARγ agonist, RSG, tips the scale in favor of PPARγ.

In a similar manner, we detected the competition between PPARγ and VDR and between VDR and RARα.

Data showed that NRs compete for RXRα and revealed differences in the binding affinities between RXRα and its partners; it was the highest to RAR, intermediate to PPARγ and the lowest to VDR. Moreover, RXR partner selection is mediated by the availability of the specific ligand, and it is dose dependent.

We also repeated the experiments transfecting less NR1 and NR2. In the new model system, RXRα is not limiting anymore; RXRα > (NR1+NR2). Data showed that overexpression of RXRα abrogates competition between its potential heterodimerization partners.

4.2. The effect of specific agonist treatment on RXR homodimerization revealed by SPIM-ALEX-FRET-FCCS

Quantitative mapping of molecular (co-)mobility by fluorescence (cross-)correlation spectroscopy (F(C)CS) in a Single Plane Illumination Microscope (SPIM) has been introduced to reveal molecular diffusion and binding. A complementary aspect of interactions is proximity, which can be studied by Förster resonance energy transfer (FRET).

To validate this concept, we acquired FRET and FCCS data with continuous excitation (cont. exc.) and with ALEX on dedicated control samples. As expected; GC^{+} dimer showed high FRET and crosscorrelation, while the GC^{-} sample had similar cross-correlation but low FRET and with G/C sample no FRET or cross-correlation were obtained.

Next, we addresssed the impact of specific agonist treatment, LG268, on RXR homodimerization. We cotransfected Hela cells with G-RXRLBD and C-RXRLBD and applied LG268. We characterized the dimerization and the chromatin binding of these LBDs via FRET and FCCS in reference to our validated control samples. These RXR-LBDs should have the capacity to heterodimerize but do not bind to DNA.

We could detect a median E value of ~3.4% in untreated cells, which increased to 5.4% upon LG268 treatment. *rCCF* increased from 0.42 to 0.61 upon LG268 treatment confirming homodimerization and its ligand-induced increase.

In conclusion, these results revealed ligand dependent homodimerization of RXR and demonstrate the advantage of SPIM-ALEX-FRET-FCCS again: the extent of dimerization may have been underestimated if applying FRET alone.

4.3. Agonist treatment enhances the specific DNA binding of VDR.

Our finding that specific agonist binding increases the affinity of the studied NRs toward RXR raises the question if it also affects their chromatin binding properties.

We applied ChIP- seq to investigate this possibility in the case of VDR. The genomic binding sites (GBSs) of VDR were detected by ChIP-seq in THP-1 macrophages. VDR occupied three types of GBSs; *i)* n_1= 1866 “VDRE”, GBSs containing a full Vitamin D response element; DR3). *ii)* n_2= 1572 less specific GBSs having a single AGGTCA sequences denoted as “NR half-site”. *iii)* n_3= 10477 GBSs where neither a VDRE nor an NR half-site sequence could be mapped, these were denoted as “None”.

Upon calcitriol activation, VDRE-containing GBSs showed considerably higher occupancies on average than in the control, untreated sample. A similar induction, but into a much lesser extent, was detected for the NR half-site-containing regions. In contrast, the "None" GBSs did not show any induction upon calcitriol.

These GBSs were further clustered according to their tag densities and response types into two clusters, and we applied *de novo* motif enrichment analysis within each group. The majority of the GBSs in the "VDRE" and NR-half sites responded positively to calcitriol treatment, and they showed enrichment with PU.1, C/EBP, and AP-1 suggesting that GBSs in cluster 1 may be enhancers. While the majority of the GBSs in the "None" group responded negatively to calcitriol treatment and the promoter specific YY1 was also enriched at these sites.

Taken all together, we can conclude that direct DNA binding (to VDREs or NR half-sites) is enhanced by calcitriol, which together with our microscopy data suggests that heterodimerization with RXR and direct DNA binding are correlated events.

4.4. Agonist treatment partially counteracts the effect of Doxorubicin on RAR mobility.

Despite the efficacy of Doxorubicin (Dox) in treating malignancies, its use has been challenged by several side effects, mainly cardiotoxicity. Several studies have attributed doxorubicin induced cardiotoxicity (DIC) to topoisomerase poisoning and reactive oxygen species, ROS, production. Furthermore, the RAR ligand ATRA has been shown to induce binding of the receptor to the Top2β promoter and down-regulate its expression levels. ATRA also reduces ROS production through activation of the ERK2 signaling pathway. These observations link Dox to RAR signaling and highlight the importance of studying the interactions between Dox and RAR.

Here we carried out FRAP experiments in Hela cells stably expressing G-RARα to track changes in RAR mobility in the nucleus at different doses of doxorubicin, in the absence or presence of specific RARα agonist (AM580).

Our data showed that with an increasing doxorubicin concentration the overall mobility of RARα increased. This is indicated by the detected reduction in the average recovery time of G-RARα. There was only a slight reduction of both the slow and fast recovery times when doxorubicin was applied at 1.25 μM. At 4.5 μM, doxorubicin reduced the recovery times by almost 50%. A further 50% reduction was detected as doxorubicin concentration increased to 18 μM. The overall mobile pool decreased from 98-100% to ~93%.

The impact of RARα specific agonist (0.1 μM AM580) was also tested along with all the tested doxorubicin concentrations. AM580 ameliorated the Dox effect only up to 4.5 μM.

To assess if the reduced recovery times observed for G-RARα reflect reduced binding or increased diffusibility, we measured the effect of Dox on the diffusion of an inert protein, a protein with no known binding sites on chromatin, the EGFP dimer, which was transfected transiently into HeLa cells. Doxorubicin treatment did not influence the diffusion of EGFP dimer indicating that doxorubicin did not alter the microviscosity in the nucleus and the reduced recovery time in the case of RAR does indeed reflect reduced DNA-binding.

To conclude, doxorubicin treatment can affect the DNA-binding of RAR, and specific agonist treatment can ameliorate this effect. This could help to design better treatment strategies that could encounter the wide range side effects caused by doxorubicin.

5. Discussion

Nuclear receptors are widely used, excellent targets for drug intervention in many diseases. However, in recent trials, unexpected side effects have been observed despite the high specificity of the drug-NR interaction. Here we propose how activation of one NR pathway can interfere indirectly with other NR pathways through competition for their heterodimeric partner RXR.

To study the interactions between NRs we applied a simple but robust assay; translocation assay applied in a three-color imaging model system.

The mutation in the NLS1 of NR1s increases their presence in the cytoplasm but retains their ability to heterodimerize with RXR and to bind their ligands effectively. According to our experiments using mutants forms of RXR we can confirm that NR1 nuclear translocation is due to heterodimerization with RXR rather than to DNA binding; RXR*nlsm* (lacking the NLS) failed to shuttle the NR1s into the nucleus while RXR*znm* (lacking the DNA binding capacity but having an NLS and heterodimerization capacity) had succeeded to do so and as effectively as the wt RXR did.

The RXR-dependent translocation of NR1 could be explained via the piggyback mechanism, which had been described for other NRs like PXR and CAR.

Tracing the dynamic distribution pattern of EGFP-VDR, EGFP-PPARγ/nlsm and EGFP-RARα/*nlsm* (homogeneous in the absence of RXRα and nuclear-enriched in response to RXRα binding) serves as a good model system for studying their competition for heterodimerization with RXRα using a simple nuclear translocation assay.

Data showed that there is indeed dynamic competition between RXR partners, which is governed by two mechanisms. First, in the absence of agonist treatment, there is a hierarchy of affinities between RXRα and its partners in the following order: RARα > PPARγ > VDR. Second, in the presence of agonist treatment, RXRα partner selection is shifted towards the liganded partner.

ChIP-seq data of VDR revealed that the specific agonist treatment increases the specific DNA-binding of VDR to its HRE, DR3. Together with the microscopy data, which showed that specific agonist treatment increases the heterodimerization with RXR, we can conclude that RXR-NR heterodimerization and direct DNA binding are correlated events, and both are augmented by specific agonist treatment. (Fig. 1)

These results may explain certain side effects of drugs targeting NRs. Competition for RXR could be responsible for the symptoms of vitamin D deficiency developed in a child upon receiving systemic retinoid treatment for ichthyosis, or the antagonistic effect of co-administered vitamin A on serum calcium response to vitamin D treatment. (Fig. 2)

Our observations regarding these three RXR partners is consistent with the regulation of metabolism in which triggering a specific metabolic pathway is dictated by the availability of the endogenous substrates. In a fast state where energy production is needed, free fatty acids, FFA, accumulates in the liver reducing the expression of genes involved in fatty acid and cholesterol synthesis while activating genes promoting fatty acid catabolism; FFA increases the expression of PPARα and evokes its transcriptional activity regulating genes involved in mitochondrial β-oxidation. On the other hand, in a fed state, with a high-fat diet, the delivery of fatty acid to the liver is decreased and the oxysterol accumulates. Oxysterol dependent activation of LXR eliminates the excess of cholesterol by increasing the expression of genes involved in bile acid synthesis, cholesterol absorption, transport and excretion. This example of regulation of metabolism by two NRs implies how the liver can avoid competition between two NRs mediating two interacting signaling pathways by providing only one partner's ligand at a specific time.

Our findings are a proof-of-concept of a hierarchy of affinities between NRs and their common partner, RXRα. It can help to explain the complex response observed in *in vivo* tests and may help design novel treatment strategies utilizing already FDA-approved drugs in an appropriate combination.

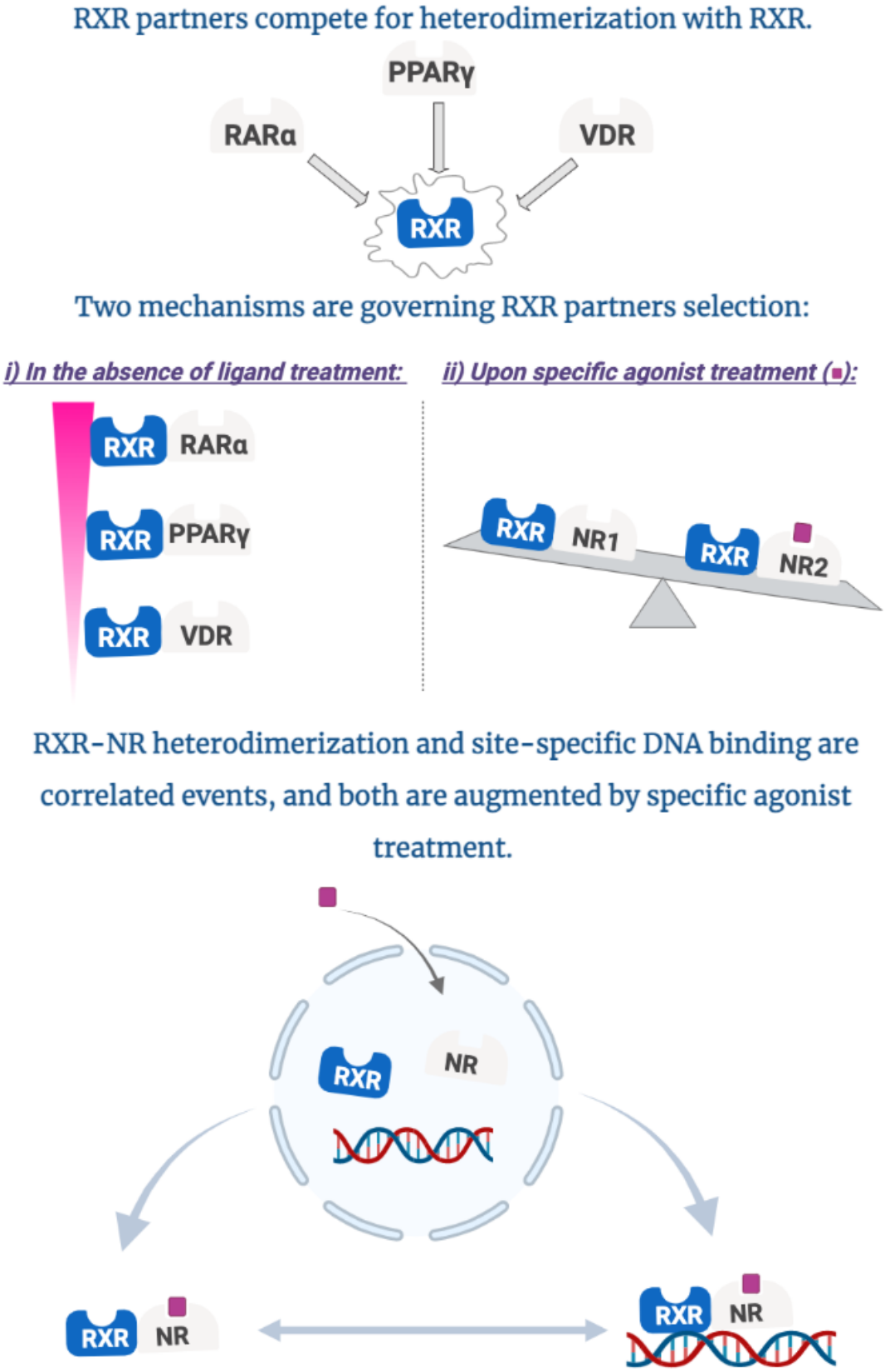

Figure 1. Schematic representation of the study results.

Possible biological consequences of the competition between NRs for a limiting pool of RXR.

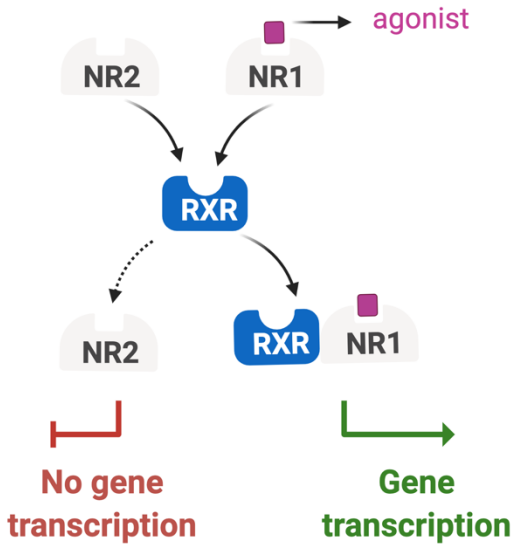

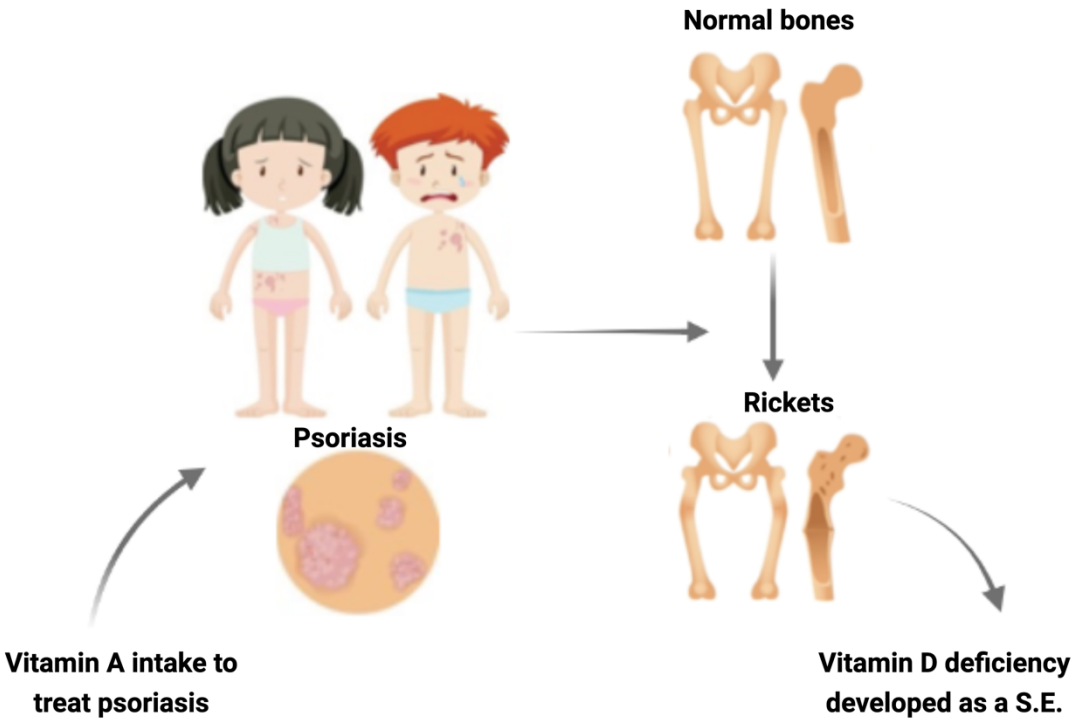

Figure 2. Schematic representation of the clinical or biological consequences of our results.

UNIVERSITY AND NATIONAL LIBRARY
UNIVERSITY OF DEBRECEN
H-4002 Egyetem tér 1, Debrecen
Phone: +3652/410-443, email: publikaciok@lib.unideb.hu

Registry number: DEENK/503/2021.PL
Subject: PhD Publication List

Candidate: Lina Fadel
Doctoral School: Doctoral School of Molecular Medicine

List of publications related to the dissertation

1. **Fadel, L.**, Rehó, B., Volkó, J., Bojcsuk, D., Kolostyák, Z., Nagy, G., Müller, G., Simándi, Z., Hegedűs, É., Szabó, G., Tóth, K., Nagy, L., Vámosi, G.: Agonist binding directs dynamic competition among nuclear receptors for heterodimerization with retinoid X receptor.
   J. Biol. Chem. 295 (29), 10045-10061, 2020.
   DOI: http://dx.doi.org/10.1074/jbc.RA119.011614
   IF: 5.157
2. Rehó, B., Lau, L., Mocsár, G., Müller, G., **Fadel, L.**, Brázda, P., Nagy, L., Tóth, K., Vámosi, G.: Simultaneous Mapping of Molecular Proximity and Comobility Reveals Agonist-Enhanced Dimerization and DNA Binding of Nuclear Receptors.
   Anal. Chem. 92 (2), 2207-2215, 2020.
   DOI: http://dx.doi.org/10.1021/acs.analchem.9b04902
   IF: 6.986

Total IF of journals (all publications): 12,143
Total IF of journals (publications related to the dissertation): 12,143

The Candidate's publication data submitted to the iDEa Tudóstér have been validated by DEENK on the basis of the Journal Citation Report (Impact Factor) database.

24 November, 2021

DEBRECENI EGYETEM * Egyetemi és Nemzeti Könyvtár *